The University of Sydney

Department of Civil Engineering
Sydney NSW 2006
AUSTRALIA

http://www.civil.usyd.edu.au/

Environmental Fluids/Wind Group

A Semi-Analytical Solution of a Circular Tunnel Surrounded by a Poroelastic Medium and Subjected to a Moving Load

Research Report No R857

Frank Jian-Fei Lu, BE EM PhD
Dong-Sheng Jeng, BE ME PhD

December 2005

The University of Sydney

Department of Civil Engineering
Environmental Fluids/Wind Group
http://www.civil.usyd.edu.au/

A Semi-Analytical Solution Of a Circular Tunnel Surrounded By a Poroelastic Medium and Subjected to a Moving Load

Research Report No R857

Frank Jian-Fei Lu, BE ME PhD
Dong-Sheng Jeng, BE ME PhD

December 2005

Abstract:
In this study**,** dynamic response of a circular tunnel embedded in a porous medium and subjected to a moving axisymmetric ring load is investigated. To avoid treating Biot's dynamic equations directly, two scalar potentials and two vector potentials are introduced to represent the displacements of the solid skeleton and the pore fluid. Based on Biot's theory and the Fourier transformation, the frequency domain governing equations for the potentials are derived. Performing the Fourier transformation on the axial coordinate, general solutions of the potentials are derived from the governing equations of the potentials. Using the obtained general solutions and boundary conditions along the tunnel surface, the boundary value problem is formulated in the frequency-wave-number domain. Solution of the boundary value problem yields the unknown constants of the potentials. The closed form solutions in the frequency-wave-number domain for the displacements, stresses and pore pressure are derived in terms of the obtained potentials. Analytical inversion of the Fourier transformation with respect to the frequency together with the numerical inversion of the Fourier transformation with respect to axial wave number leads to the numerical solutions of the displacements, stresses and pore pressure. For demonstration of our method, some numerical examples and corresponding analysis are given in the paper.

Keywords:
porous media; tunnel; moving loads; Biot's theory; the Fourier transformation

Copyright Notice

Department of Civil Engineering, Research Report R857
A Semi-Analytical Solution of a Circular Tunnel Surrounded by a Poroelastic Medium and Subjected to a Moving Load

f.lu@civil.usyd.edu.au d.jeng@civil.usyd.edu.au

Published by:
Department of Civil Engineering
The University of Sydney
Sydney NSW 2006
AUSTRALIA

December 2005

This report and other Research Reports published by The Department of Civil Engineering are available on the Internet:

http://www.civil.usyd.edu.au

Contents

1 Introduction[1]

Prompted by the popularity of high-speed trains and magnetically levitated trains, many researchers recently have been focusing on the interaction between high-speed load and surrounding media. For example, Gonzalez and Abascal (2004) developed a boundary element method for moving loads in a linear visco-elasticity. Using time domain Green's function, Rasmussen et al (2001) established a time domain boundary element method for moving load problems of an isotropic elastic media. A layered half-space subjected to a moving periodic load as well as a trainload was investigated by Grundmann et al (1999). A comprehensive review and treatment of moving load problems were presented by Fryba (1999). It should be noted that for high-speed trains and magnetically levitated trains, the speed of the train is very close to Rayleigh wave speeds or shear wave speeds of saturated soft soils. Consequently, it is crucial to analyze the dynamic interaction between high-speed vehicles and the surrounding saturated porous media. As a result, moving load problems for saturated porous media has begun to attract the interest of some investigators. For instance, Burke and Kingsbury (1984) presented a closed-form analytical solution for a poroelastic medium subjected to a traveling surface pressure. Siddharthan et al (1993) studied the dynamic response of a layered poroelastic half-space by solving Biot's dynamic fundamental equations approximately. Jin et al (2004) presented a semi-analytical treatment of a 2D half-plane porous media subjected to a surface-moving line load.

A circular tunnel subjected to a moving load is of fundamental importance for transportation engineering and mining engineering as well as geophysical exploration. For example, the noise and vibration generated by a moving vehicle inside a tunnel is crucial for the design of a tunnel; the dynamic interaction between the gas detonation wave inside a mine and surrounding rocks is important in evaluating the damage caused by gas explosions. To date, there have been many researches regarding the analysis of a circular tunnel subjected to dynamic or static load. For example, Jordan (1962) investigated the dynamic problem of a circular borehole subjected to an explosive pressure over a segment of the surface of the hole. Using dynamic elasticity theory and the Fourier transformation, the response of an infinite elastic medium to a traveling load in a cylindrical borehole was presented by Parnes (1969). Parnes (1983, 1986) also studied the dynamic response of a circular borehole loaded by a harmonic normal ring load and a harmonic torsional ring force. Later, Metrikine and

[1] This report is part of the manuscript: Lu, J.-F. and Jeng, D-S. (2005) A semi-analytical solution of a circular tunnel surrounded by a poroelastic medium and subjected to a moving load. *Acta Mechanics* (submitted)

Vrouwenvelder (2000) put forward an approximate two-dimensional model for the evaluation of surface ground vibration due to moving vehicles inside a tunnel. There are a few researches concerning the qusai-static analysis of a circular tunnel embedded in a poroelastic medium. For example, based on Biot's consolidation theory as well as the Laplace and the Fourier transformation method, a circular borehole embedded in a poroelastic medium subjected to a static ring load was addressed by Rajapakse (1993). Using decomposition scheme, poroelastic solution for an inclined borehole was presented in Cui et al. (1997). However, as for a circular tunnel in a poroelastic medium subjected to a moving ring load, no research has been carried out so far.

In this study, the Biot's dynamic theory (Bio, 1956a, b, 1962) will be used to analyse dynamic responses of a porous medium to a moving ring load inside a circular tunnel. Two scalar potentials and two vectorial potentials are introduced to represent the displacements of the solid skeleton and the pore fluid, and the frequency domain governing equations for the potentials are derived. Through the Fourier transformation on the axial coordinate, the general solutions for the potentials in cylindrical coordinate system are derived from the governing equations of the potentials. The closed-form solutions for the displacements, stresses and pore pressure in the frequency-wave-number domain are obtained in terms of the obtained potentials. Analytical inversion of the Fourier transformation with respect to the frequency together with the numerical inversion of the Fourier transformation with respect to axial wave number leads to the numerical solutions of the displacements, stresses and pore pressure for the porous medium. To demonstrate the proposed method, some numerical examples and corresponding parametric analysis are given in the paper.

2 Governing equations and general solutions

2.1 Biot's theory and definition of the Fourier transformation

The constitutive equations for homogeneous porous medium have the form (Biot, 1956a, b, 1962)

$$\sigma_{ij} = 2\mu\varepsilon_{ij} + \lambda\delta_{ij}e - \alpha\delta_{ij}p\,, \tag{1}$$

$$p = -\alpha Me + M\vartheta\,, \tag{2}$$

where ε_{ij}, e are the strain tensor and the dilatation of the solid skeleton; ϑ is the volume of fluid injected into unit volume of bulk material; σ_{ij} is the stress of bulk material; p is the excess pore fluid pressure and δ_{ij} is the Kronecker delta. Moreover, λ, μ are Lame constants of the solid skeleton; α, M are Biot parameters (Biot, 1941) accounting for the compressibility of the saturated porous medium. Note that $0 \le \alpha \le 1, 0 \le M < \infty$, and for completely dry materials $M \to 0$, for materials with incompressible constituents $\alpha \to 1, M \to \infty$.

In (1) and (2), the dilatation of the solid skeleton e and the volume of fluid injected into unit volume of bulk material ϑ are defined as

$$e = u_{i,i}, \ \vartheta = -w_{i,i}, \ w_i = \phi(U_i - u_i), \tag{3}$$

where u_i and U_i denote the average solid displacement and the fluid displacement, and ϕ is the porosity of material. The expression for the fluid discharge in *i*-th ($i = x, y, z$) direction has the following form

$$q_i = \frac{\partial w_i}{\partial t}. \tag{4}$$

The equation of motion for the bulk material and the pore fluid are expressed in terms of the displacements u_i and w_i

$$\mu u_{i,jj} + (\lambda + \alpha^2 M + \mu) u_{j,ji} + \alpha M w_{j,ji} = \rho_b \ddot{u}_i + \rho_f \ddot{w}_i, \tag{5a}$$

$$\alpha \ M u_{j,ji} + M w_{j,ji} = \rho_f \ddot{u}_i + m \ddot{w}_i + \frac{\eta}{k} K(t) * \dot{w}_i, \tag{5b}$$

where ρ_b, ρ_f denote the bulk density of the porous medium and the density of the pore fluid, $\rho_b = (1-\phi)\rho_s + \phi\rho_f$, ρ_s is the density of the solid skeleton and ϕ is the porosity of the porous medium; $m = a_\infty \rho_f / \phi$ and a_∞ is tortuosity; η, k account for the viscosity of the pore fluid and the permeability of the porous medium, respectively and $K(t)$ is a time dependent viscosity correction factor which describes the transition behavior from viscosity dominated flow in the low frequency range towards inertia dominated flow at high frequency range (Biot, 1962b; Johnson et al., 1987; Pride et al., 199); a superimposed dot on a variable

denotes the derivative with respect to time and a star between two variables denotes time convolution.

For convenience of the following analysis, a reference length, reference shear modulus and reference density a_R, μ_R, ρ_R are introduced in the paper. All the geometrical and physical quantities are non-dimensionalized as follows

$$x_i^* = \frac{x_i}{a_R}, u_i^* = \frac{u_i}{a_R}, w_i^* = \frac{w_i}{a_R}, q_i^* = q_i\sqrt{\frac{\rho_R}{\mu_R}}, \eta^* = \frac{\eta}{a_R\sqrt{\mu_R\rho_R}}, k^* = \frac{k}{a_R^2}, \lambda^* = \frac{\lambda}{\mu_R}, \mu^* = \frac{\mu}{\mu_R},$$

$$M^* = \frac{M}{\mu_R}, F^* = \frac{F}{\mu_R a_R^2}, \rho_b^* = \frac{\rho_b}{\rho_R}, \rho_f^* = \frac{\rho_f}{\rho_R}, t^* = \frac{t}{a_R}\sqrt{\frac{\mu_R}{\rho_R}}, \ \omega^* = \omega a_R\sqrt{\frac{\rho_R}{\mu_R}}, \tag{6}$$

where the quantities with asterisk are the non-dimensional quantities and F denotes force. In the remainder of this paper, the non-dimensional geometrical and physical quantities in Eq. (6) will be used. Furthermore, for simplicity, the superscript asterisks will be omitted in all the quantities in what follows.

To derive the general solutions for Biot's equations in the cylindrical coordinate system, two kinds of Fourier transformation are involved: the Fourier transformation with respect to time and frequency and the Fourier transformation with respect to axial coordinate and axial wave number. In this study, the Fourier transformation for the both cases is defined as follows

$$\hat{f}(\delta) = \int_{-\infty}^{+\infty} f(x)e^{-i\delta x}dx, \ f(x) = \frac{1}{2\pi}\int_{-\infty}^{+\infty}\hat{f}(\delta)e^{i\delta x}d\tau, \tag{7}$$

where x denotes time or space coordinate, while δ represents frequency or axial wave number, $i = \sqrt{-1}$.

2.2 The potentials for Biot's theory

To solve the Biot equations, the Helmholtz decomposition for the solid displacement and the fluid displacement is introduced. In Cartesian coordinate system *xyz*, therefore, the displacement of the solid skeleton and the pore fluid have the following form

$$u_i = \varphi_{,i}^{(s)} + e_{ijk}\psi_{k,j}^{(s)} \tag{8a}$$

$$w_i = \varphi^{(f)}_{,i} + e_{ijk}\psi^{(f)}_{k,j} \tag{8b}$$

where $\varphi^{(s)}, \psi^{(s)}_k, k = 1,2,3$ are the scalar and vectorial potentials for the solid displacement, while $\varphi^{(f)}, \psi^{(f)}_k, k = 1,2,3$ are those for the pore fluid and e_{ijk} is the Levi-Civita symbol.

Substitution of (8) into (5) and applying the Fourier transformation to time variable yields

$$(\lambda_c + 2\mu)\hat{\varphi}^{(s)}_{,jj} + \rho_b\omega^2\hat{\varphi}^{(s)} = -\alpha M\hat{\varphi}^{(f)}_{,jj} - \rho_f\omega^2\hat{\varphi}^{(f)} \tag{9a}$$

$$\alpha^2 M\hat{\varphi}^{(s)}_{,jj} + \alpha\rho_f\omega^2\hat{\varphi}^{(s)} = -\alpha M\hat{\varphi}^{(f)}_{,jj} - \alpha\beta_1\hat{\varphi}^{(f)} \tag{9b}$$

$$\hat{\psi}^{(s)}_{k,jj} + k_t^2\hat{\psi}^{(s)}_k = 0 \tag{9c}$$

$$\hat{\psi}^{(f)}_k = \beta_2\hat{\psi}^{(s)}_k \tag{9d}$$

where the superimposed symbol $\wedge$ above a variable denote the Fourier transformation with respect to time, $\lambda_c = \lambda + \alpha^2 M$, $\beta_1 = m\omega^2 - i(\eta/k)\omega\hat{K}(\omega)$, $\beta_2 = -\rho_f\omega^2/\beta_1$ and k_t is the frequency-dependent complex wave number for the shear wave of the porous medium

$$k_t = \omega\sqrt{\frac{\rho_b + \beta_2\rho_f}{\mu}}. \tag{10}$$

Note that to guarantee the attenuation of elastic wave in the porous medium, the imaginary part of k_t should be non-positive for the Fourier transformation defined in (7). Combination of (9a) and (9b) gives the following expressions

$$\hat{\varphi}^{(f)} = \frac{\lambda + 2\mu}{\beta_3}\hat{\varphi}^{(s)}_{,jj} + \frac{\rho_b\omega^2 - \alpha\rho_f\omega^2}{\beta_3}\hat{\varphi}^{(s)} \tag{11a}$$

$$\hat{\varphi}^{(s)}_{,jjkk} + \varepsilon_1\hat{\varphi}^{(s)}_{,jj} + \varepsilon_2\hat{\varphi}^{(s)} = 0 \tag{11b}$$

where $\varepsilon_1 = (\delta_2 + \delta_3 + \lambda_c + 2\mu)/\delta_1$, $\varepsilon_2 = (\delta_4 + \rho_b\omega^2)/\delta_1$, $\delta_1 = \alpha M(\lambda + 2\mu)/\beta_3$, $\delta_2 = \alpha M(\rho_b\omega^2 - \alpha\rho_f\omega^2)/\beta_3$, $\delta_3 = \rho_f\omega^2(\lambda + 2\mu)/\beta_3$, $\delta_4 = \rho_f\omega^2(\rho_b\omega^2 - \alpha\rho_f\omega^2)/\beta_3$, $\beta_3 = \alpha\beta_1 - \rho_f\omega^2$.

Eqs. (9) and (11) indicate that the potentials of the solid and the pore fluid are not independent: the potentials of the pore fluid can be derived from those of the solid skeleton. Moreover, the vectorial potential for the solid frame is determined by the Helmholtz equation (9c), which can be easily solved in cylindrical coordinate system by the Fourier transformation. In order to develop the general solution for the potential $\hat{\varphi}^{(s)}$, Eq.(11b) is rewritten in the following form

$$(\nabla^2 + k_f^2)(\nabla^2 \hat{\varphi}^{(s)} + k_s^2 \hat{\varphi}^{(s)}) = 0 \tag{12}$$

where ∇^2 is the Laplacian operator, $k_f^2 + k_s^2 = \varepsilon_1$, $k_f^2 k_s^2 = \varepsilon_2$, k_f, k_s are the frequency-dependent complex wave numbers for the fast and slow P wave, respectively. If introducing potential $\hat{\chi}$, Eq.(12) is reduced to

$$\nabla^2 \hat{\varphi}^{(s)} + k_s^2 \hat{\varphi}^{(s)} = \hat{\chi} \tag{13a}$$

$$\nabla^2 \hat{\chi} + k_f^2 \hat{\chi} = 0 \tag{13b}$$

It follows from Eq.(13), the general solution of the potential $\hat{\chi}$ is given by the Helmholtz equation (13b), while the general solution of $\hat{\varphi}^{(s)}$ is given by the inhomogeneous Helmholtz equation (13a).

2.3 General solutions in an axisymmetric cylindrical coordinate system

Since the moving ring load is axisymmetric, thus, it is convenient to consider our problem in cylindrical coordinate system (ρ, θ, z). If an axisymmetric condition is taken into account,

the vectorial potential $\hat{\psi}_k^{(s)}$ and $\hat{\psi}_k^{(f)}$ in the coordinate system (ρ,θ,z) can be represented by one scalar potential. Therefore, the displacements for the solid skeleton and pore fluid are expressed as follows

$$\hat{u}_\rho = \frac{\partial \hat{\varphi}^{(s)}}{\partial \rho} + \frac{\partial^2 \hat{\eta}^{(s)}}{\partial \rho \partial z},\ \hat{u}_z = \frac{\partial \hat{\varphi}^{(s)}}{\partial z} - \frac{1}{\rho}\frac{\partial}{\partial \rho}\left(\rho \frac{\partial \hat{\eta}^{(s)}}{\partial \rho}\right), \tag{14a}$$

$$\hat{w}_\rho = \frac{\partial \hat{\varphi}^{(f)}}{\partial \rho} + \frac{\partial^2 \hat{\eta}^{(f)}}{\partial \rho \partial z},\ \hat{w}_z = \frac{\partial \hat{\varphi}^{(f)}}{\partial z} - \frac{1}{\rho}\frac{\partial}{\partial \rho}\left(\rho \frac{\partial \hat{\eta}^{(f)}}{\partial \rho}\right) \tag{14b}$$

where ρ, z are radial and axial coordinate, respectively (Figure 1), $\hat{\varphi}^{(s)}$, $\hat{\varphi}^{(f)}$ are given by Eqs.(11), (13), while the potentials $\hat{\eta}^{(s)}$, $\hat{\eta}^{(f)}$ are determined by the following equations

$$\nabla^2 \hat{\eta}^{(s)} + k_t^2 \hat{\eta}^{(s)} = 0 \tag{15a}$$

$$\hat{\eta}^{(f)} = \beta_2 \hat{\eta}^{(s)} \tag{15b}$$

where the axisymmetric Laplacian operator is defined by $\nabla^2 = \partial^2/\partial\rho^2 + 1/\rho\partial/\partial\rho + \partial^2/\partial^2 z$.

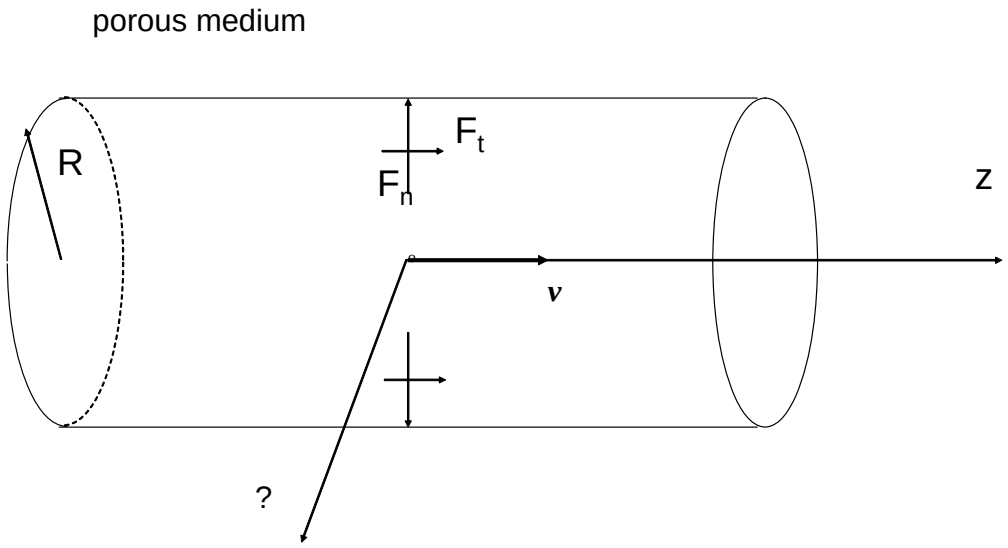

Figure 1 A circular tunnel in a porous medium subjected to a moving ring concentrated or distributed load.

Performing the Fourier transformation with respect to axial coordinate z on Eq. (13b), one has

$$\frac{\partial^2 \tilde{\chi}}{\partial \rho^2} + \frac{1}{\rho}\frac{\partial \tilde{\chi}}{\partial \rho} + (k_f^2 - \xi^2)\tilde{\chi} = 0 \tag{16}$$

where the superimposed tilde denotes the combination of the Fourier transformation with respect to time and the Fourier transformation with respect to axial coordinate z, ξ is the axial wave number. Letting $\gamma_f^2 = k_f^2 - \xi^2$ and choosing the branch of γ_f to satisfy $\mathrm{Im}(\gamma_f) < 0$, then the general solution of Eq. 16) has the form

$$\tilde{\chi} = A(\omega, \xi) H_0^{(2)}(\gamma_f \rho) \tag{17}$$

in which $A(\omega,\xi)$ is a arbitrary constant to be determined by boundary conditions, $H_0^{(2)}(\bullet)$ denotes the second kind of the Hankel function of zero order. Similarly, performing the Fourier transformation to coordinate z on Eq.(13a) leads to

$$\frac{\partial^2 \tilde{\phi}^{(s)}}{\partial \rho^2}+\frac{1}{\rho}\frac{\partial \tilde{\phi}^{(s)}}{\partial \rho}+(k_s^2-\xi^2)\tilde{\phi}^{(s)}=\tilde{\chi} \tag{18}$$

Using solution (17), the general solution for Eq.(18) is obtained as follows

$$\tilde{\phi}^{(s)}=\frac{A(\omega,\xi)}{k_s^2-k_f^2}H_0^{(2)}(\gamma_f\rho)+B(\omega,\xi)H_0^{(2)}(\gamma_s\rho) \tag{19}$$

where $\gamma_s^2=k_s^2-\xi^2$ and $\mathrm{Im}(\gamma_s)<0$, $B(\omega,\xi)$ is a arbitrary constant. Applying the Fourier transformation to coordinate z on Eq. (15a) yields the general solution for $\tilde{\eta}^{(s)}$

$$\tilde{\eta}^{(s)}=C(\omega,\xi)H_0^{(2)}(\gamma_t\rho) \tag{20}$$

where $\gamma_t^2=k_t^2-\xi^2$ with $\mathrm{Im}(\gamma_t)<0$ and $C(\omega,\xi)$ is a arbitrary constant. In terms of Eqs.(11a), (15b), (19), (20), the general solutions for the potentials of the pore fluids have the following forms

$$\tilde{\phi}^{(f)}=\frac{\alpha_2-\alpha_1 k_f^2}{k_s^2-k_f^2}A(\omega,\xi)H_0^{(2)}(\gamma_f\rho)+(\alpha_2-\alpha_1 k_s^2)B(\omega,\xi)H_0^{(2)}(\gamma_s\rho) \tag{21a}$$

$$\tilde{\eta}^{(f)}=\beta_2 C(\omega,\xi)H_0^{(2)}(\gamma_t\rho) \tag{21b}$$

where $\alpha_1=(\lambda+2\mu)/\beta_3$, $\alpha_2=(\rho\omega^2-\alpha\rho_f\omega^2)/\beta_3$.

It is noted that the displacement of the solid frame and the pore fluid as well as the stresses and pore pressure can be further obtained from the displacement-potential relations and the constitutive relations for the porous medium. The expressions for the displacements, stresses and the pore pressure are as follows

$$\tilde{u}_\rho=\frac{\gamma_f\ A(\omega,\xi)}{k_f^2-k_s^2}H_1^{(2)}(\gamma_f\rho)-\gamma_s B(\omega,\xi)\,H_1^{(2)}(\gamma_s\rho)-i\xi\gamma_t C(\omega,\xi)\,H_1^{(2)}(\gamma_t\rho) \tag{22a}$$

$$\tilde{u}_z = \frac{i\xi\ A(\omega,\xi)}{k_s^2 - k_f^2} H_1^{(2)}(\gamma_f \rho) + i\xi\ B(\omega,\xi)\ H_0^{(2)}(\gamma_s \rho) + \gamma_t^2\ C(\omega,\xi)\ H_0^{(2)}(\gamma_t \rho) \tag{22b}$$

$$\tilde{w}_\rho = \frac{(\alpha_2 - \alpha_1 k_f^2)\gamma_f A(\omega,\xi)}{k_f^2 - k_s^2} H_1^{(2)}(\gamma_f \rho) - (\alpha_2 - \alpha_1 k_s^2)\gamma_s\ B(\omega,\xi)\ H_1^{(2)}(\gamma_s \rho)$$

$$- i\xi\ \beta_2\ \gamma_t\ C(\omega,\xi) H_1^{(2)}(\gamma_t \rho) \tag{22c}$$

$$\tilde{w}_z = i\xi[\frac{(\alpha_2 - \alpha_1 k_f^2)A(\omega,\xi)}{k_s^2 - k_f^2} H_0^{(2)}(\gamma_f \rho) + (\alpha_2 - \alpha_1 k_s^2)B(\omega,\xi)H_0^{(2)}(\gamma_s \rho)]$$

$$+ \frac{\beta_2 \gamma_t C(\omega,\xi)}{\rho} H_1^{(2)}(\gamma_t \rho) + \beta_2\ \gamma_t^2\ C(\omega,\xi)\ [H_0^{(2)}(\gamma_t \rho) - \frac{1}{\rho \gamma_t} H_1^{(2)}(\gamma_t \rho)] \tag{22d}$$

$$\tilde{\sigma}_{\rho\rho} = 2\mu[\frac{\gamma_f^2 A(\omega,\xi)}{k_s^2 - k_f^2} H_0^{(2)}(\gamma_f \rho) - \frac{\gamma_f A(\omega,\xi)}{\rho(k_s^2 - k_f^2)} H_1^{(2)}(\gamma_f \rho) - \gamma_s^2 B(\omega,\xi)H_0^{(2)}(\gamma_s \rho)$$

$$+ \frac{\gamma_s B(\omega,\xi)}{\rho} H_1^{(2)}(\gamma_s \rho) - i\xi\gamma_t^2 C(\omega,\xi)H_0^{(2)}(\gamma_t \rho) + \frac{i\xi\gamma_t C(\omega,\xi)}{\rho} H_1^{(2)}(\gamma_t \rho)] +$$

$$\lambda[\frac{k_f^2 A(\omega,\xi)}{k_f^2 - k_s^2} H_0^{(2)}(\gamma_f \rho) - k_s^2 B(\omega,\xi)H_0^{(2)}(\gamma_s \rho)] \tag{22e}$$

$$\tilde{\sigma}_{z\rho} = \frac{\mu}{k_f^2 - k_s^2}[2\mathrm{i}\xi\gamma_f A(\omega,\xi)H_1^{(2)}(\gamma_f \rho) + 2\mathrm{i}\xi\gamma_s k_s^2 B(\omega,\xi)H_1^{(2)}(\gamma_s \rho) -$$

$$- 2i\xi\gamma_s k_f^2 B(\omega,\xi)H_1^{(2)}(\gamma_s \rho) - \xi^2\gamma_t k_s^2 C(\omega,\xi)H_1^{(2)}(\gamma_t \rho) + \xi^2\gamma_t k_f^2 C(\omega,\xi)H_1^{(2)}(\gamma_t \rho)$$

$$+ \gamma_t^3 k_s^2 C(\omega,\xi)H_1^{(2)}(\gamma_t \rho) - \gamma_t^3 k_f^2 C(\omega,\xi)H_1^{(2)}(\gamma_t \rho)] \tag{22f}$$

$$\tilde{\sigma}_{\theta\theta} = \frac{2\mu}{\rho}[\frac{\gamma_f A(\omega,\xi)}{k_f^2 - k_s^2} H_1^{(2)}(\gamma_f \rho) - \gamma_s B(\omega,\xi)H_1^{(2)}(\gamma_s \rho) - \mathrm{i}\xi\gamma_t C(\omega,\xi)H_1^{(2)}(\gamma_t \rho)]$$

$$+ \lambda[\frac{k_f^2 A(\omega,\xi)}{k_f^2 - k_s^2} H_0^{(2)}(\gamma_f \rho) - k_s^2 B(\omega,\xi)H_0^{(2)}(\gamma_s \rho)] \tag{22g}$$

$$\tilde{p} = \frac{\alpha M\ k_s^2 A(\omega,\xi)}{k_s^2 - k_f^2} H_0^{(2)}(\gamma_f \rho) + \alpha M\ k_s^2 B(\omega,\xi)H_0^{(2)}(\gamma_s \rho)$$

$$+\frac{M\,k_f^2(\alpha_2-\alpha_1 k_f^2)A(\omega,\xi)}{k_s^2-k_f^2}H_0^{(2)}(\gamma_f\rho)-M(\alpha_2-\alpha_1 k_s^2)k_s^2\;B(\omega,\xi)H_0^{(2)}(\gamma_s\rho) \quad (22h)$$

3 Boundary value problems and the corresponding solutions

A circular tunnel with radius R embedded in an infinite isotropic porous medium is investigated in this paper (Figure 1). The surface of the circular tunnel is subjected to a moving normal or a tangent axisymmetric ring load, which can be either concentrated load along a circle or a uniformly distributed load over a segment of the tunnel surface. Using the general solutions derived in the above section and the boundary conditions along the tunnel surface, boundary value problems can be formulated in frequency-wave-number domain. Solution of the boundary value problems yields the three arbitrary constants involved in the general solutions.

If a moving concentrated normal or tangent ring load F_n, F_t with velocity v is applied on the tunnel surface, then, the boundary conditions have the following form

$$\sigma_{\rho\rho}(R,z,t)=-\frac{F_n}{2\pi R}\delta(z-vt) \quad (23a)$$

$$\sigma_{z\rho}(R,z,t)=-\frac{F_t}{2\pi R}\delta(z-vt) \quad (23b)$$

where $\delta(\bullet)$ is the Dirac-δ function. On the other hand, if the moving load is distributed over a segment of length $2d$, then, the boundary conditions can be expressed as follows

$$\sigma_{\rho\rho}(R,z,t)=-p_n[H(z-vt+d)-H(z-vt-d)] \quad (24a)$$

$$\sigma_{z\rho}(R,z,t)=-p_t[H(z-vt+d)-H(z-vt-d)] \quad (24b)$$

where $H(\bullet)$ is the Heaviside function and p_n, p_t is the intensities of the normal and tangent traction applied on the tunnel surface.

If the tunnel surface is completely permeable, the pore pressure at the tunnel surface should vanish

$$p(R,z,t)=0 \tag{25}$$

On the contrary, if the tunnel surface is fully impermeable, then, the following boundary condition holds

$$q_\rho(R,z,t)=\frac{\partial w_\rho(R,z,t)}{\partial t}=0 \tag{26}$$

Performing double Fourier transformation with respect to t,z on Eq. (23), the corresponding boundary conditions in the frequency-wave-number domain are obtained as follows

$$\tilde{\sigma}_{\rho\rho}(R,\xi,\omega)=-\frac{F_n}{R}\delta(\omega+\xi v) \tag{27a}$$

$$\tilde{\sigma}_{z\rho}(R,\xi,\omega)=-\frac{F_t}{R}\delta(\omega+\xi v) \tag{27b}$$

Similarly, double Fourier transformation of Eq (24) leads to the following boundary conditions in the frequency-wave-number domain

$$\tilde{\sigma}_{\rho\rho}(R,\xi,\omega)=-4\pi p_n\delta(\omega+\xi \mathrm{v})\frac{\sin(\xi \mathrm{d})}{\xi} \tag{28a}$$

$$\tilde{\sigma}_{z\rho}(R,\xi,\omega)=-4\pi p_t\delta(\omega+\xi \mathrm{v})\frac{\sin(\xi \mathrm{d})}{\xi} \tag{28b}$$

Likewise, in the frequency-wave-number domain, the permeable and impermeable boundary conditions have the forms

$$\tilde{p}(R,\xi,\omega)=0 \tag{29a}$$

$$\tilde{q}_\rho(R,\xi,\omega)=i\omega\tilde{w}_\rho(R,\xi,\omega)=0 \tag{29b}$$

By using Eqs. (27) or (28), (29) and Eq.(22), the arbitrary constants $A(\omega,\xi)$, $B(\omega,\xi)$, $C(\omega,\xi)$ in Eq.(22) can be calculated. Due to the limitation of this paper, the expressions of the arbitrary constants for all the cases will not be listed here. However, for the concentrated ring normal load F_n ($F_t=0$), the expressions for the three arbitrary constants $A(\omega,\xi)$, $B(\omega,\xi)$, $C(\omega,\xi)$ are given in the Appendix. Note that the three arbitrary constants for other cases can be calculated according to the above procedure in a straightforward way.

Substituting the obtained constants $A(\omega,\xi)$, $B(\omega,\xi)$, $C(\omega,\xi)$ into Eq. (22), the displacements, stresses and pore pressure in the frequency-wave-number domain are obtained. The time-space domain solution can be recovered by double inverse Fourier transformation with respect to ω,ξ, respectively. It is worth noting that due to the presence of the factor $\delta(\omega+\xi \mathrm{v})$ in all the terms of the expressions for the displacements, stresses and pore pressure, consequently, the inverse Fourier transformation with respect to frequency ω can be fulfilled analytically (Eason, 1965). However, as the expressions for the displacements, stresses and pore pressure are very complicated, the inverse Fourier transformation with respect to axial wave number ξ can only be implemented by a numerical method.

To show the implementation of the double inverse Fourier transformation to the physical quantities in Eq.(22), we shall use $\tilde{\Omega}$ to denote all the physical variables. Suppose the tunnel is subjected to a moving concentrated normal ring load, then, the expression of $\tilde{\Omega}$ can always be written as follows

$$\tilde{\Omega}(\rho,\xi,\omega) = -\frac{F_n}{R}\delta(\omega+\xi v)\tilde{\Omega}^*(\rho,\xi,\omega) \tag{30}$$

The integral representation of $\Omega(\rho,z,t)$ in the time-space domain has the following form

$$\Omega(\rho,z,t) = -\frac{F_n}{R}\left(\frac{1}{2\pi}\right)^2 \int_{-\infty}^{+\infty}\int_{-\infty}^{+\infty} \delta(\omega+\xi v)\tilde{\Omega}^*(\rho,\xi,\omega)e^{i(\omega t+\xi z)}d\omega d\xi \tag{31}$$

Using the property of the Dirac-δ function, the above integral can be reduced to

$$\Omega(\rho,z,t) = -\frac{F_n}{R}\left(\frac{1}{2\pi}\right)^2 \int_{-\infty}^{+\infty} \tilde{\Omega}^*(\rho,\xi,-\xi v)e^{i\xi(z-vt)}d\xi\,. \tag{32}$$

As mentioned above, due to the complexity of the integrand in (32), $\Omega(\rho,z,t)$ can only be evaluated via numerical approach. Moreover, it follows from Eq. (32) that if let $z' = z - vt$, $\Omega(\rho,z,t)$ will become time-independent and it only depends on z',ρ, which means if a moving reference frame (ρ,θ,z') is attached on the moving load, the response of the porous medium measured in the moving reference frame is time-independent. Physically, this point is equivalent to the fact that if a load has been moving for a very long time, then, a steady state will be achieved in the moving reference frame adhered to the moving load.

4 Numerical results and corresponding analysis

The general solutions of the problem listed in (22) consist of three arbitrary constants. After determining the constants by solving the boundary value problems, the solution in the time-space domain is represented by infinite integral (32). Since the drag force between the solid skeleton and the pore fluid is dissipative, all the branch points and the pole, which corresponds to the pseudo-Rayleigh wave along the surface of the tunnel, of the expression $\Pi(\xi,\omega)$ (see Appendix) are complicated. Thus, the infinite integral (32) with respect to the axial wave number ξ are free of any singularities in the path of integration. The numerical integration in (32), therefore, can be calculated directly by subroutine DQDAGI, which is available in IMSL library.

It follows from (23) and (24), a moving load along the surface of the tunnel is of Dirac or Heaviside type. Consequently, high frequency components are involved in the response spectrum of the porous medium. Therefore, the low frequency Biot's theory (Biot, 1962a) is not suitable for the present problem. To characterize the high frequency drag force between the solid skeleton and the pore fluid, the JKD model (Johnson et al., 1987) is incorporated with Biot's theory (Biot, 1956b) in the present research. The JKD model can give an adequate approximation for many porous media (Johnson et al., 1987; Pride et al., 1993). The complex frequency dependent viscosity correction function in the JKD model has the form (Johnson et al., 1987)

$$\hat{K}(\omega) = (1 + i\frac{\omega}{\omega_c}\alpha_g)^{1/2},\ \omega_c = \frac{\eta\phi}{\rho_f a_\infty k} \tag{33}$$

where ω_c is transition frequency which separates viscous-force-dominated flow from inertial-force-dominated flow and α_g is the pore geometry term which is commonly equal to ½ for many porous media (Johnson et al., 1987; Pride et al., 1993).

In addition, in the following calculations, the reference length, reference shear modulus and reference density a_R, μ_R, ρ_R are chosen as follows

$$a_R = R,\ \mu_R = \mu,\ \rho_R = \rho_f \tag{34}$$

4.1 Dynamic response of the points with $-7.5 \le z' \le 7.5$ *and* ρ=1.5

In this section, the dynamic response of the points with $-7.5 \le z' = z - vt \le 7.5$ and $\rho = 1.5$ for different load velocity is calculated. The material parameters are chosen as follows: $\mu = 1.0,\ \lambda = 0.3333,\ \rho_s = 2.0,\ \rho_f = 1.0,\quad \phi = 0.3,\quad \alpha = 0.95, M = 1.67,\quad \eta = 5.774 \times 10^{-10}$, $k = 1.0 \times 10^{-13},\ \phi = 0.3$. The radius of the tunnel is $R = 1.0$ and its surface is assumed to be permeable. Three cases corresponding to $v/v_{SH} = 0.1$, $v/v_{SH} = 0.5$ and $v/v_{SH} = 0.9$ are calculated, where v_{SH} is defined as $v_{SH} = \sqrt{\mu/\rho_b}$. The moving loads are normal and tangent concentrated ring force with magnitudes, F_n, F_t, respectively and located at $z' = 0$. Figures 2 and 3 show the variation of $u_r, u_z, \sigma_{\theta\theta}, p$ versus axial coordinate z' for the normal and tangent moving concentrated ring load, respectively.

Figure 2 shows for the moving normal load, all the values of $u_r, u_z, \sigma_{\theta\theta}, p$ increase with increasing load velocity. It should be noted that the differences between the values of $u_r, u_z, \sigma_{\theta\theta}, p$ for the case of $v/v_{SH} = 0.1$ and the case $v/v_{SH} = 0.5$ are smaller than those between the case $v/v_{SH} = 0.5$ and the case $v/v_{SH} = 0.9$, which is due to the fact that $v/v_{SH} = 0.1$ and $v/v_{SH} = 0.5$ are far smaller than the velocity of the shear wave velocity of the porous medium, while $v/v_{SH} = 0.9$ is near the shear wave velocity of the porous medium. Moreover, since the velocity v/v_{SH} in this example is smaller than those of S wave and P waves of the porous medium, the Mach cones corresponding to the S wave and the P waves of the porous medium have not occurred. The values of $u_r, u_z, \sigma_{\theta\theta}, p$ are therefore nearly symmetric with respect to the load ($z' = 0$). It follows form Figure2 (d), positive pore pressure only occurs in the domain near the concentrated ring load, while for the domain far form the concentrated ring load, negative pore pressure appears. The above phenomenon can be explained by the following fact: the domain near the concentrated ring load is under compression, while the region far from the concentrated ring load is under tension. Figure3 indicates again that the values of $u_r, u_z, \sigma_{\theta\theta}, p$ for the tangent moving load increase with increasing velocity and the dynamic response of the porous medium are nearly asymmetric with respect to the load ($z' = 0$). Also, the pore pressure ahead of the moving load is always positive, while the pore pressure behind the moving load is negative.

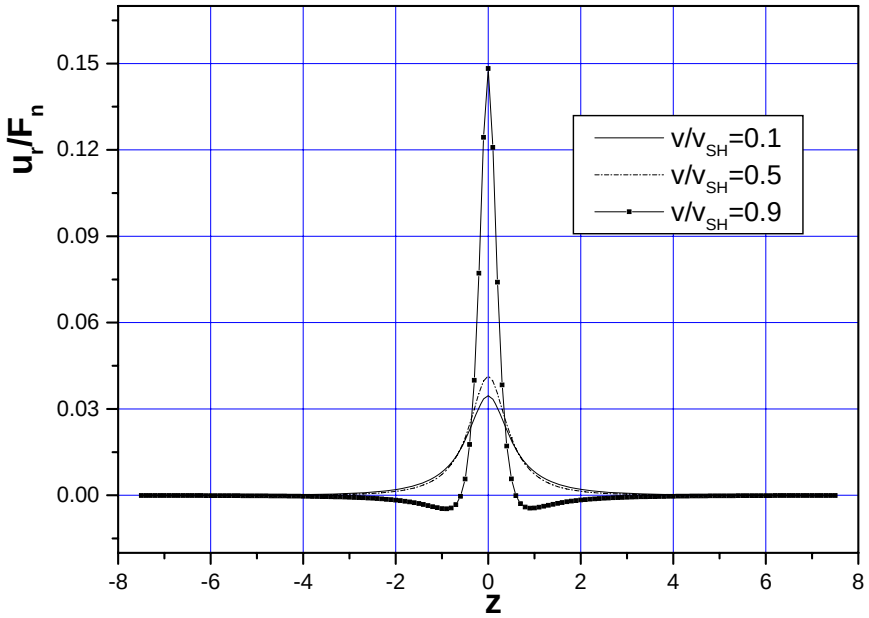
0.15
0.12
0.09
0.06
0.03
0.00
u_r/F_n
-8
-6
-4
-2
0
2
4
6
8
z
v/v_{SH}=0.1
v/v_{SH}=0.5
v/v_{SH}=0.9

(a)

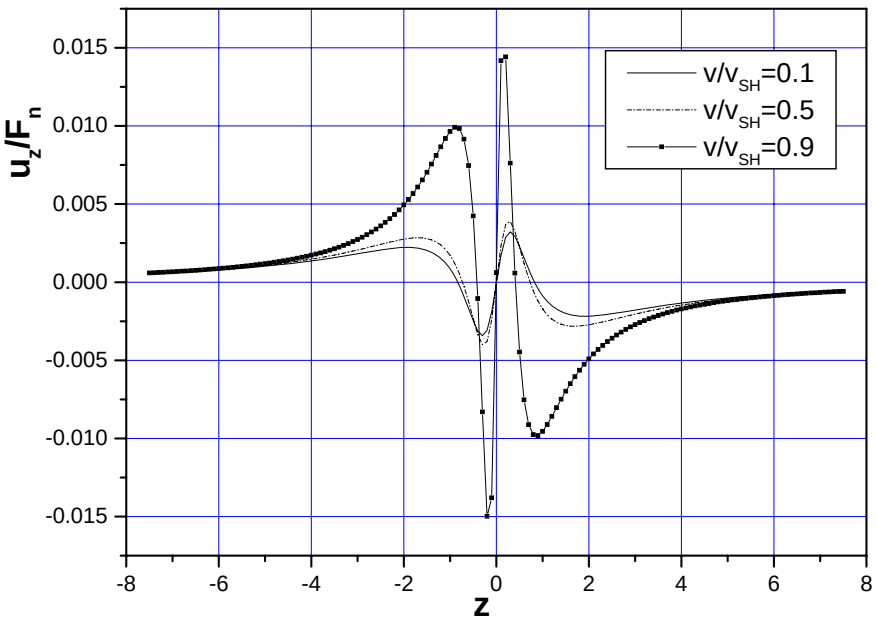
0.015
0.010
0.005
0.000
-0.005
-0.010
-0.015
u_z/F_n
-8
-6
-4
-2
0
2
4
6
8
z
v/v_{SH}=0.1
v/v_{SH}=0.5
v/v_{SH}=0.9

(b)

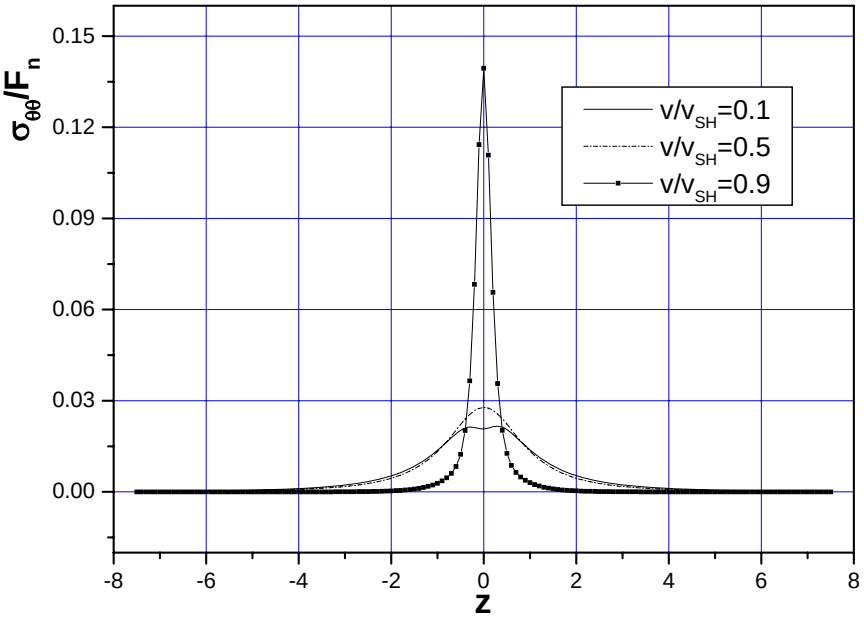

(c)

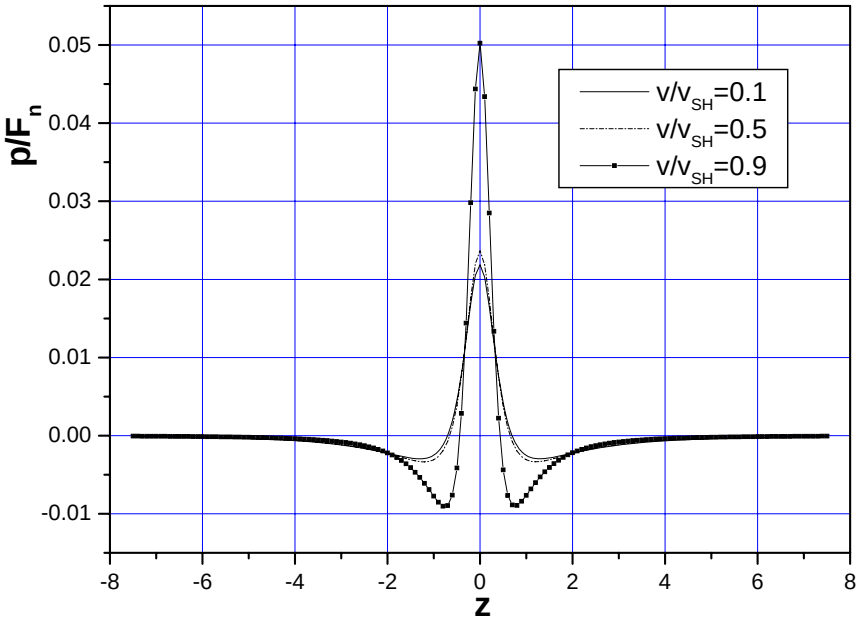

(d)

Figure 2: Dynamic response of the points with $-7.5 \le z' \le 7.5$ and $\rho = 1.5$ near a permeable circular tunnel subjected to a moving normal concentrated ring load F_n with velocity $v/v_{SH} = 0.1, 0.5, 0.9$, respectively: (a) radial displacement u_r / F_n; (b) axial displacement u_z / F_n; (c) hoop stress $\sigma_{\theta\theta} / F_n$; (d) pore pressure p / F_n.

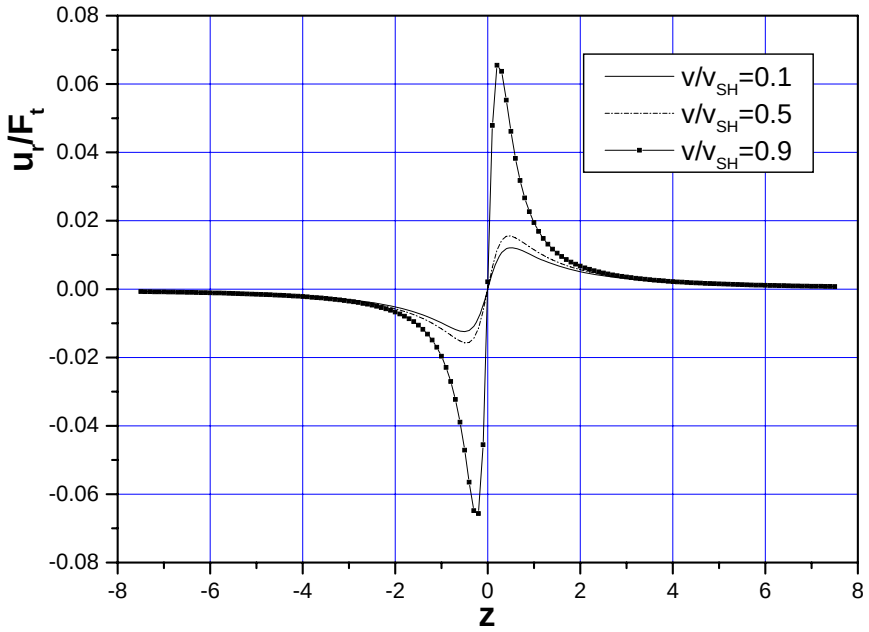
0.08
0.06
0.04
0.02
0.00
-0.02
-0.04
-0.06
-0.08
u_r/F_t
-8
-6
-4
-2
0
2
4
6
8
z
v/v_{SH}=0.1
v/v_{SH}=0.5
v/v_{SH}=0.9

(a)

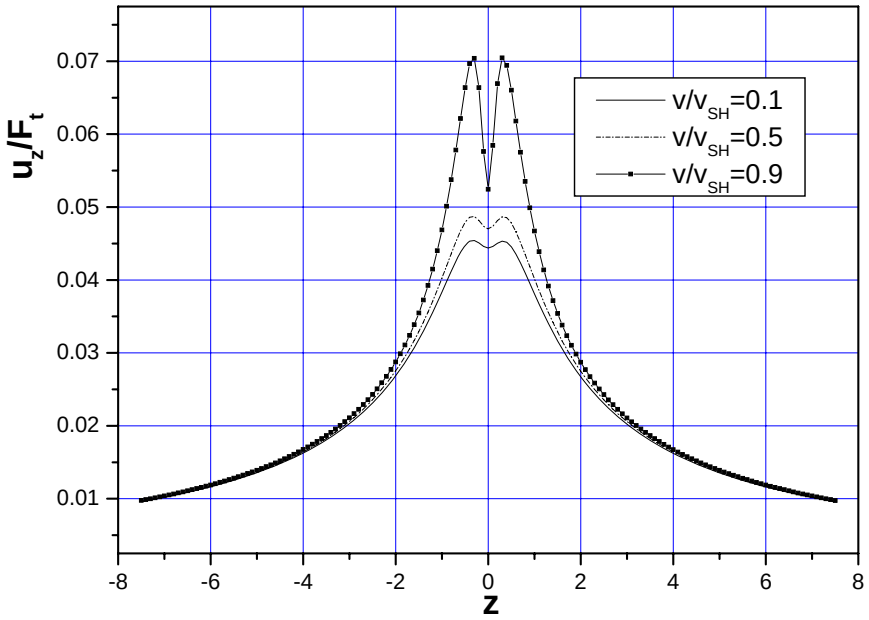
0.07
0.06
0.05
0.04
0.03
0.02
0.01
u_z/F_t
-8
-6
-4
-2
0
2
4
6
8
z
v/v_{SH}=0.1
v/v_{SH}=0.5
v/v_{SH}=0.9

(b)

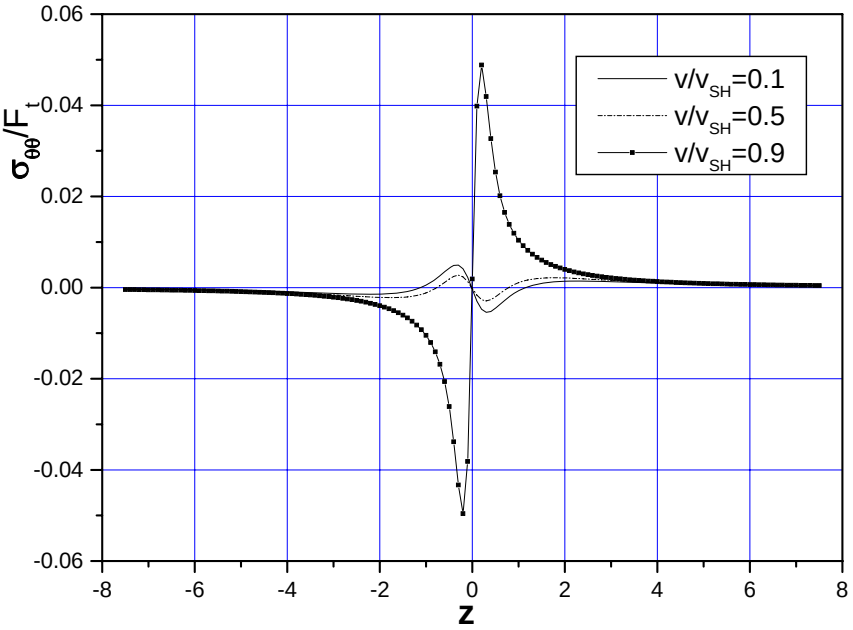

(c)

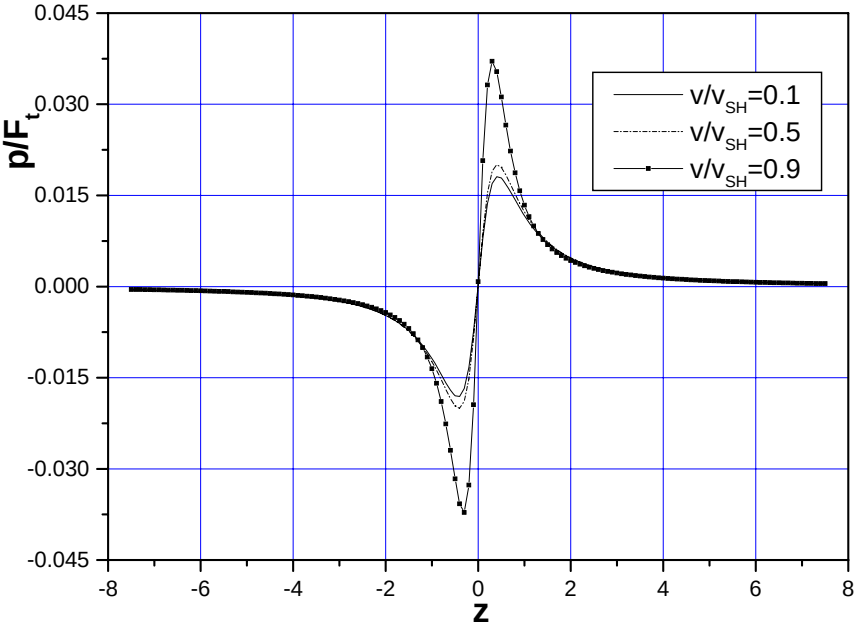

(d)

Figure 3: Dynamic response of the points with $-7.5 \le z' \le 7.5$ and $\rho = 1.5$ near a permeable circular tunnel subjected to a moving tangent concentrated ring load F_t with velocity $v/v_{SH} = 0.1, 0.5, 0.9$, respectively: (a) radial displacement u_r / F_t; (b) axial displacement u_z / F_t; (c) hoop stress $\sigma_{\theta\theta} / F_t$; (d) pore pressure p / F_t.

4.2 The influence of the load velocity on the dynamic response

In this section, the influence of the load velocity on the dynamic response of three different points with $z' = z - vt = -1.0, 0.0, 1.0$ and $\rho = 1.5$ is considered. The moving loads are normal and tangent uniformly distributed ring force over segment $-1 \le z' \le 1$ of the tunnel surface and with intensities p_n, p_t, respectively. The velocity of normal and tangent load varies from $v/v_{SH} = 0$ to $v/v_{SH} = 1.95$, where v_{SH} is defined as $v_{SH} = \sqrt{\mu/\rho_b}$. The material parameters are chosen as follows: $\mu = 1.0$, $\lambda = 0.3333$, $\rho_s = 2.0$, $\rho_f = 1.0$, $\phi = 0.3$, $\alpha = 0.95$, $M = 1.67$, $\eta = 5.774 \times 10^{-10}$, $k = 1.0 \times 10^{-14}$, $\phi = 0.3$. The radius of the tunnel is $R = 1.0$ and its surface is assumed to be permeable. Figure 4 and Figure 5 give the values of $u_r, u_z, \sigma_{\theta\theta}, p$ for the normal and tangent load at the three different points versus the load velocity.

It follows from Figure 4 that at lower load velocity, the values of $u_r, u_z, \sigma_{\theta\theta}$ at the three different points increase slightly with the increases of the velocity, while the values of p almost keep constant when $v/v_{SH} \le 0.9$. However, when the velocity approaches v_{SH}, all the values of $u_r, u_z, \sigma_{\theta\theta}, p$ increase dramatically. Furthermore, they exhibit an oscillating characteristic when v is around v_{SH}. But when the velocity is larger than v_{SH}, the response of the porous medium varies smoothly. Figure4 also shows that when the velocity of the load is lower than v_{SH}, the response of the porous medium is nearly symmetric with respect to the central of the normal load ($z' = 0$), however, when the velocity of the load tends to v_{SH}, the symmetry is damaged. It is worth noting that when the velocity of the load is around v_{SH}, the radial displacement at $z' = 1.0$ is negative (Figure 4(a)). Also, an interesting phenomenon is that when velocity $v/v_{SH} \approx 1.42$, all the pore pressures in three points vanish. Figure5 shows that at lower velocity, the response of the porous medium is asymmetric with respect to the central of the tangent load ($z' = 0$). Similarly, this asymmetry is damaged by the larger velocity of the tangent load. It follows from Figure 5(c) that at lower velocity, the value of $\sigma_{\theta\theta}$ is very small, but when v/v_{SH} is larger than 0.5, $\sigma_{\theta\theta}$ increases significantly. Figure 5(d) indicates that the pore pressure at $z' = -1.0$ is always negative and the pore pressure at $z' = 1.0$ is always positive, while the pore pressure at $z' = 0.0$ vanish when $v/v_{SH} \le 0.9$ and it

changes sign several times when $v/v_{SH} > 0.9$.

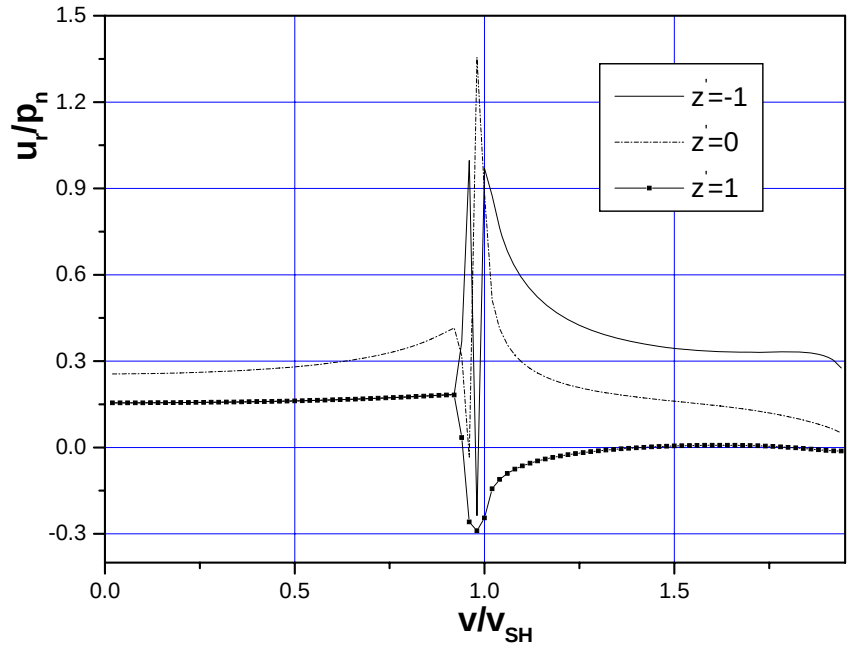

(a)

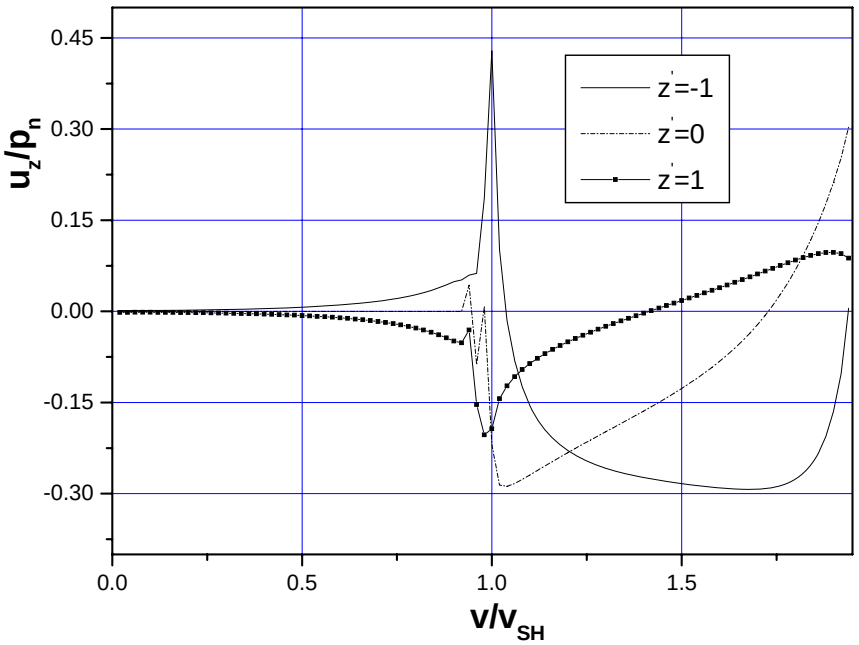

(b)

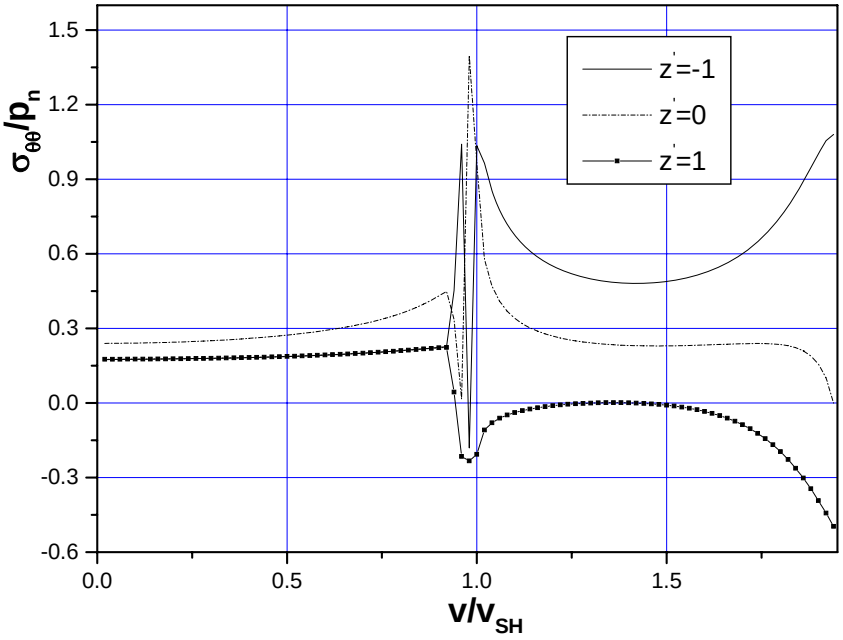

(c)

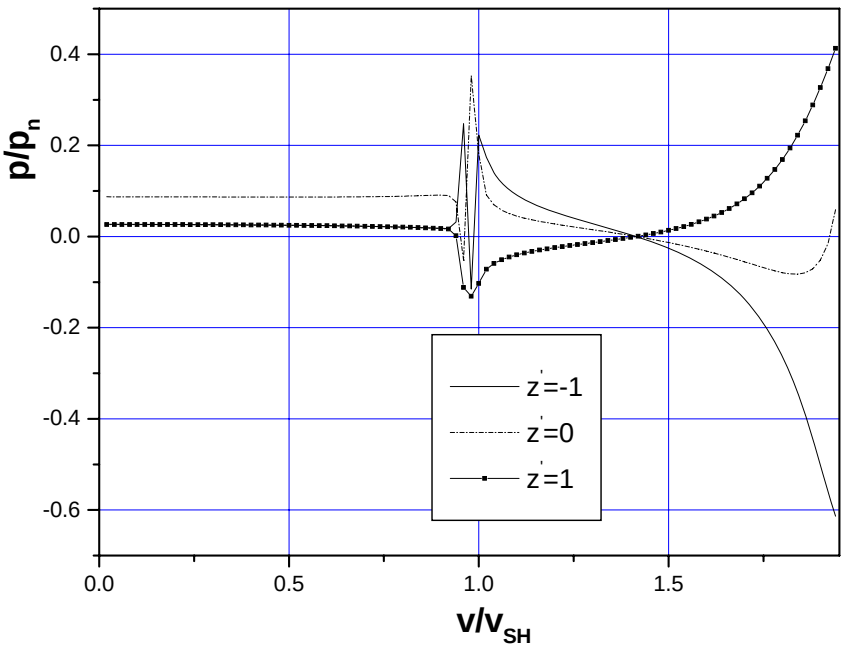

(d)

Figure 4: Dynamic response of three points with $z' = -1.0, 0.0, 1.0$ and $\rho = 1.5$ near a permeable circular tunnel subjected to a moving normal distributed ring load $p_n (-1.0 \le z' \le 1.0)$ with velocity ranging from $v/v_{SH} = 0.0$ to $v/v_{SH} = 1.95$: (a) radial displacement u_r / p_n; (b) axial displacement u_z / p_n; (c) hoop stress $\sigma_{\theta\theta} / p_n$; (d) pore pressure p / p_n.

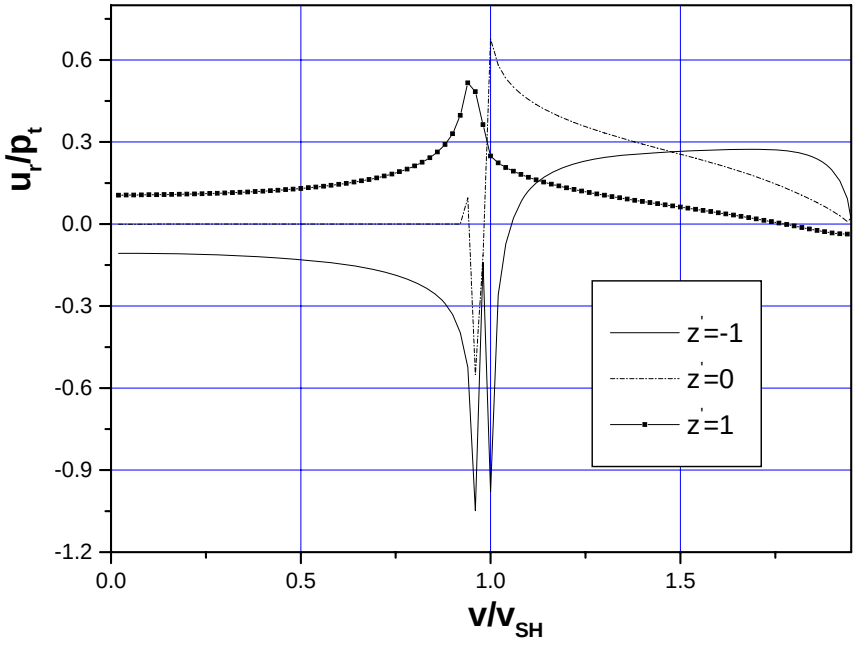
0.6
0.3
0.0
-0.3
-0.6
-0.9
-1.2
0.0
0.5
1.0
1.5
u_r/p_t
v/v_{SH}
z'=-1
z'=0
z'=1

(a)

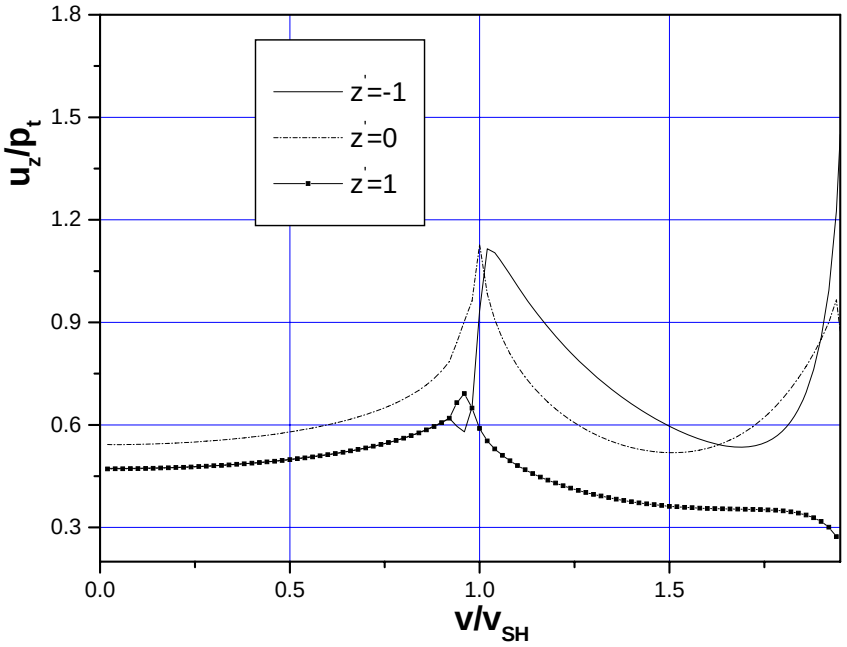
1.8
1.5
1.2
0.9
0.6
0.3
0.0
0.5
1.0
1.5
u_z/p_t
v/v_{SH}
z'=-1
z'=0
z'=1

(b)

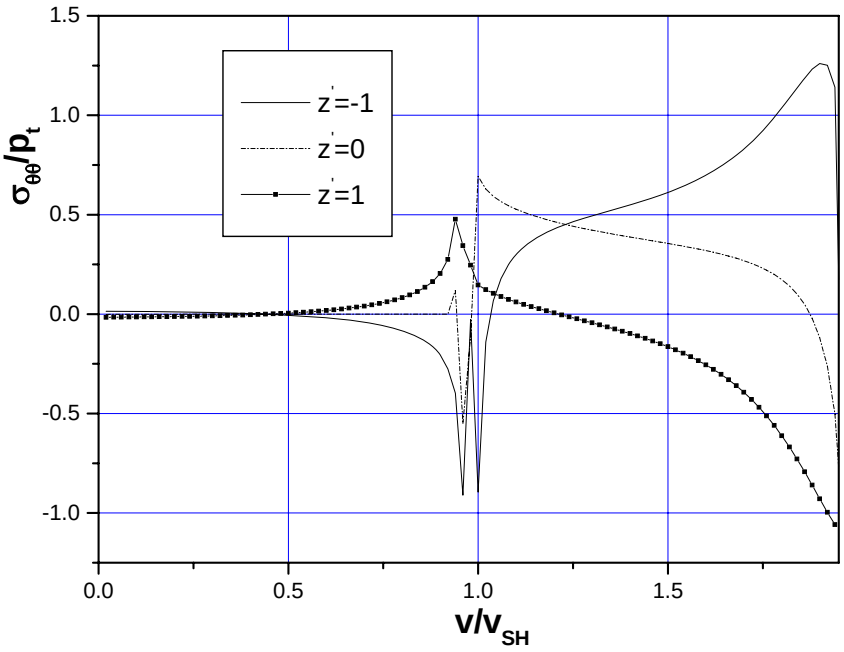

(c)

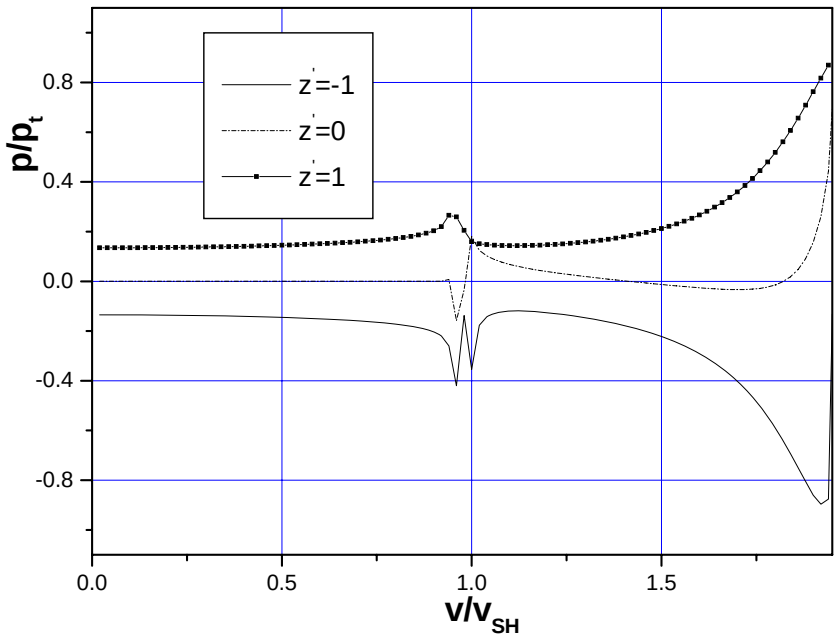

(d)

Figure 5: Dynamic response of three points with $z' = -1.0, 0.0, 1.0$ and $\rho = 1.5$ near a permeable circular tunnel subjected to a moving tangent distributed ring load $p_t (-1.0 \le z' \le 1.0)$ with velocity ranging from $v/v_{SH} = 0.0$ to $v/v_{SH} = 1.95$: (a) radial displacement u_r / p_t; (b) axial displacement u_z / p_t; (c) hoop stress $\sigma_{\theta\theta} / p_t$; (d) pore pressure p / p_t.

4.3 The influence of the boundary conditions on dynamic responses

In this section, the influence of the boundary conditions on dynamic responses of two points with coordinates $z' = z - vt = -1.0, 1.0$ and $\rho = 1.5$ is considered. Two kinds of boundary conditions– fully permeable and fully impermeable– are used in this section. The tunnel is subjected to a moving normal and tangent concentrated ring load located at $z' = 0$ and with magnitudes F_n, F_t, respectively. The velocity of the moving normal and tangent load varies from $v/v_{SH} = 0.0$ to $v/v_{SH} = 1.0$, where v_{SH} is defined as $v_{SH} = \sqrt{\mu/\rho_b}$. The material parameters are chosen as follows: $\mu = 1.0, \lambda = 0.3333, \rho_s = 2.0, \rho_f = 1.0$, $\phi = 0.3$, $\alpha = 0.95, M = 1.67$, $\eta = 5.774 \times 10^{-10}$, $k = 1.0 \times 10^{-11}$, $\phi = 0.3$, $R = 1.0$. Figure6 and Figure7 give the values of $u_r, u_z, \sigma_{\theta\theta}, p$ for the two points under permeable and impermeable boundary condition versus the velocity of the moving loads.

The plots show that the boundary conditions have minor influence on the dynamic response of the point $z' = 1$. The boundary condition has a slight influence on the displacement u_z at the point $z' = -1$ too. However, when the load velocity approaches v_{SH}, the influence of the boundary condition on the displacement u_r and stress $\sigma_{\theta\theta}$ of the point $z' = -1$ is pronounced. Figures 6 and 7 demonstrate the boundary conditions have influence on the pore pressure at the point $z' = -1$ for all the values of the velocity. It follows from Figure 6(d) that at the point $z' = -1$, the pore pressure of the impermeable boundary is larger than that of the permeable case at lower velocity; when $v/v_{SH} > 0.1$, the pore pressure of the permeable case is larger than that of the impermeable case; when v/v_{SH} approaching 1.0, again, the pore pressure of the impermeable case is larger than that of the permeable case. For the tangent load (Figure 7(d)), the pore pressure of the impermeable case is larger than that of the permeable case when $v/v_{SH} < 0.48$; however, when $v/v_{SH} > 0.48$, the pore pressure of the impermeable case is smaller than that of the permeable case.

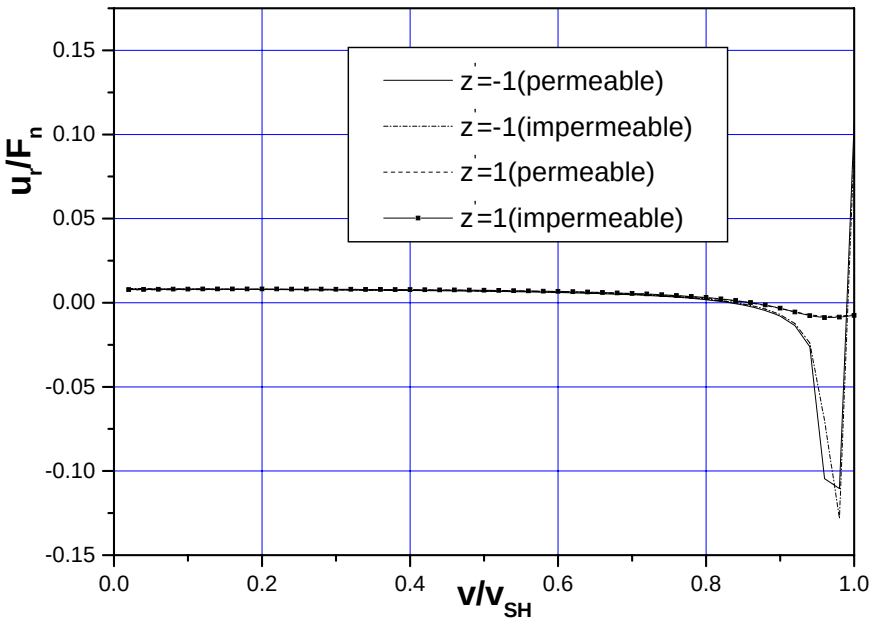
0.15
0.10
0.05
0.00
-0.05
-0.10
-0.15
0.0
0.2
0.4
0.6
0.8
1.0
u_r/F_n
v/v_{SH}
z'=-1(permeable)
z'=-1(impermeable)
z'=1(permeable)
z'=1(impermeable)

(a)

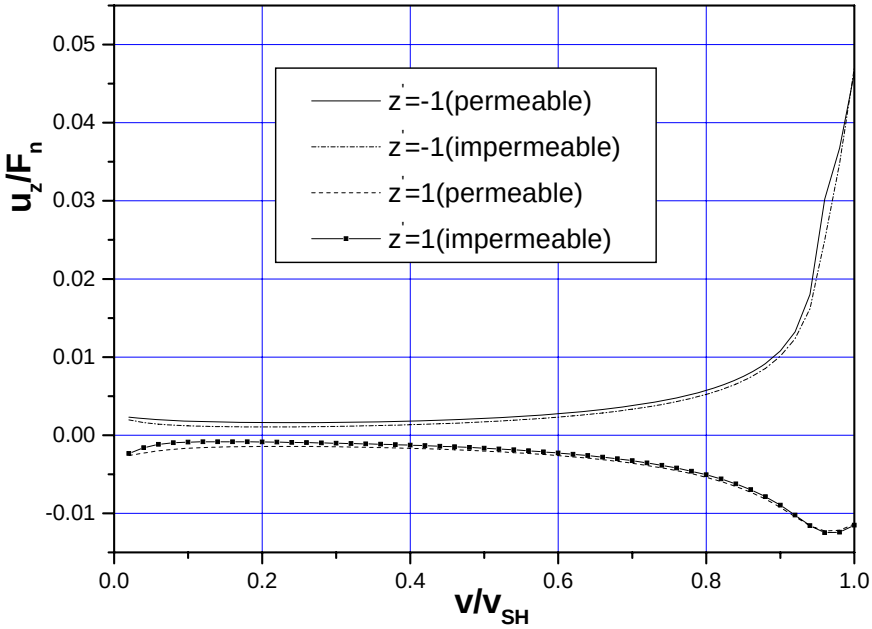
0.05
0.04
0.03
0.02
0.01
0.00
-0.01
0.0
0.2
0.4
0.6
0.8
1.0
u_z/F_n
v/v_{SH}
z'=-1(permeable)
z'=-1(impermeable)
z'=1(permeable)
z'=1(impermeable)

(b)

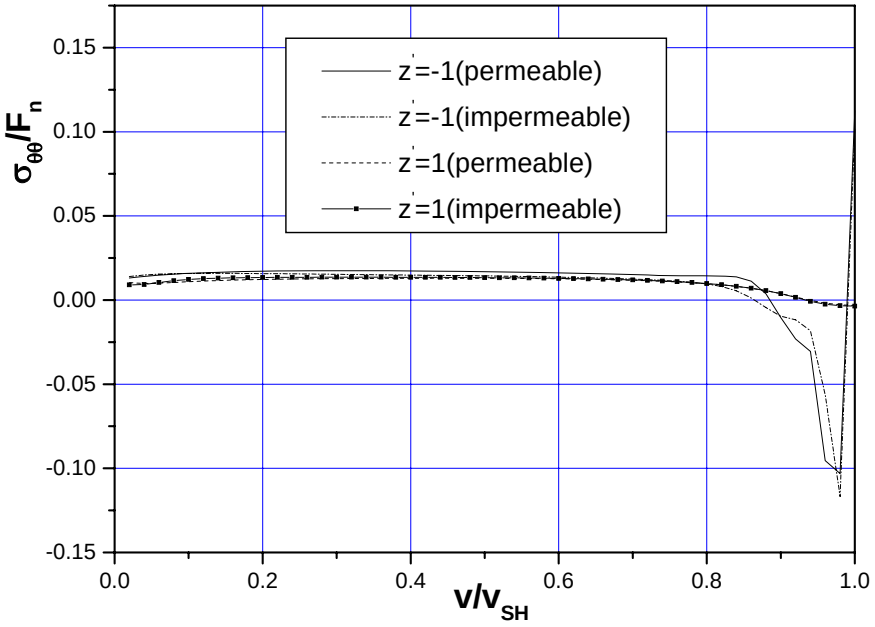

(c)

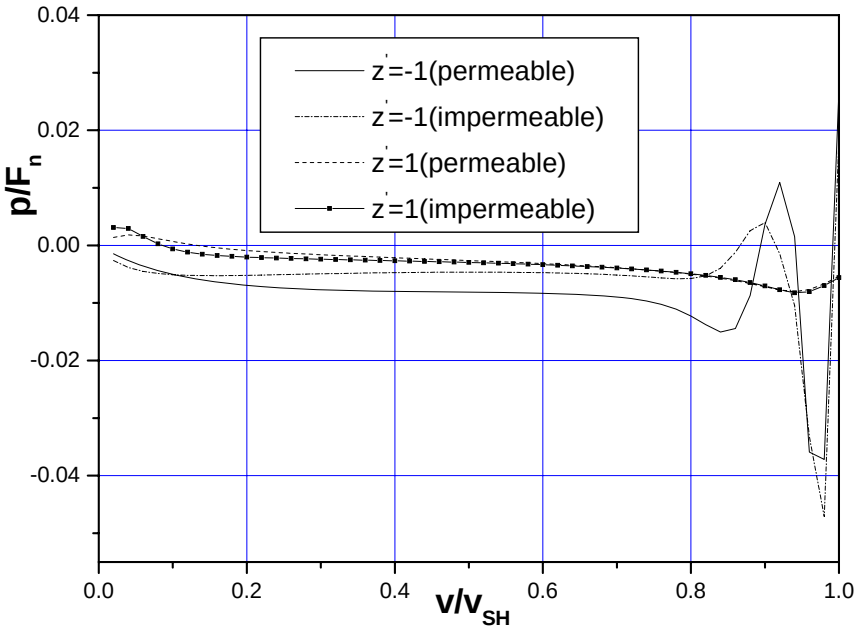

(d)

Figure 6: Dynamic response of two points with $z' = -1.0, 1.0$ and $\rho = 1.5$ near a permeable or an impermeable circular tunnel subjected to a moving normal concentrated ring load F_n with velocity ranging from $v/v_{SH} = 0.0$ to $v/v_{SH} = 1.0$: (a) radial displacement u_r / F_n; (b) axial displacement u_z / F_n; (c) hoop stress $\sigma_{\theta\theta} / F_n$; (d) pore pressure p / F_n.

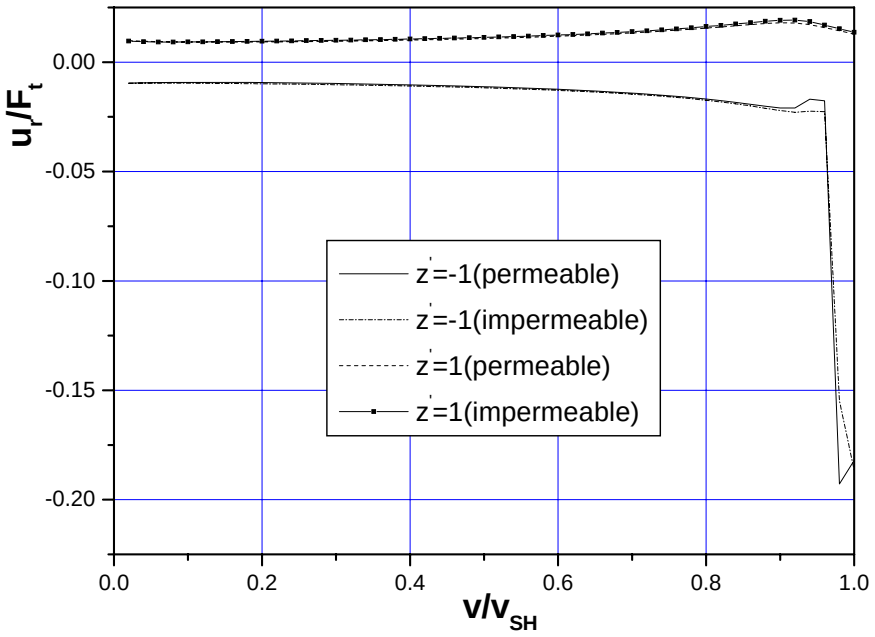
0.00
-0.05
-0.10
-0.15
-0.20
0.0
0.2
0.4
0.6
0.8
1.0
u_r/F_t
v/v_{SH}
z'=-1(permeable)
z'=-1(impermeable)
z'=1(permeable)
z'=1(impermeable)

(a)

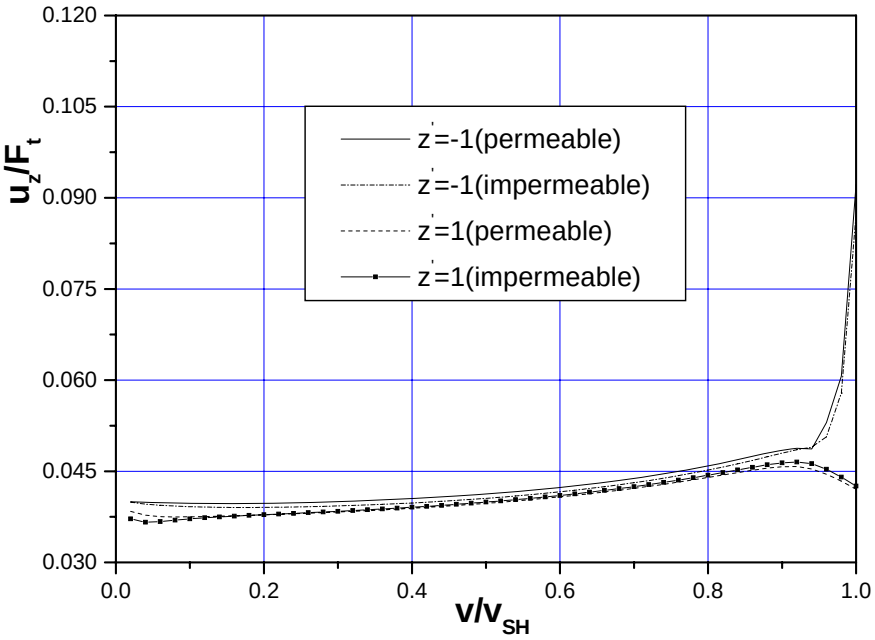
0.120
0.105
0.090
0.075
0.060
0.045
0.030
0.0
0.2
0.4
0.6
0.8
1.0
u_z/F_t
v/v_{SH}
z'=-1(permeable)
z'=-1(impermeable)
z'=1(permeable)
z'=1(impermeable)

(b)

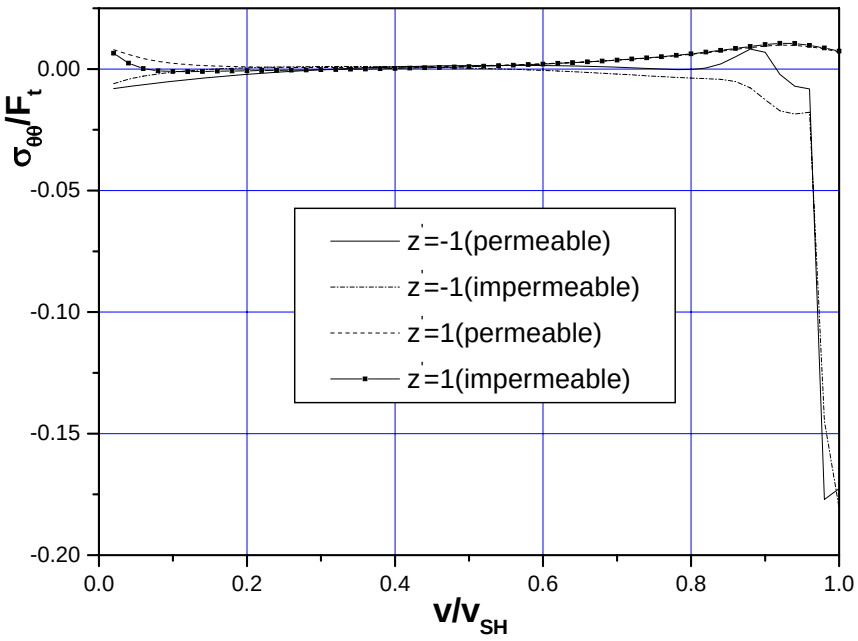

(c)

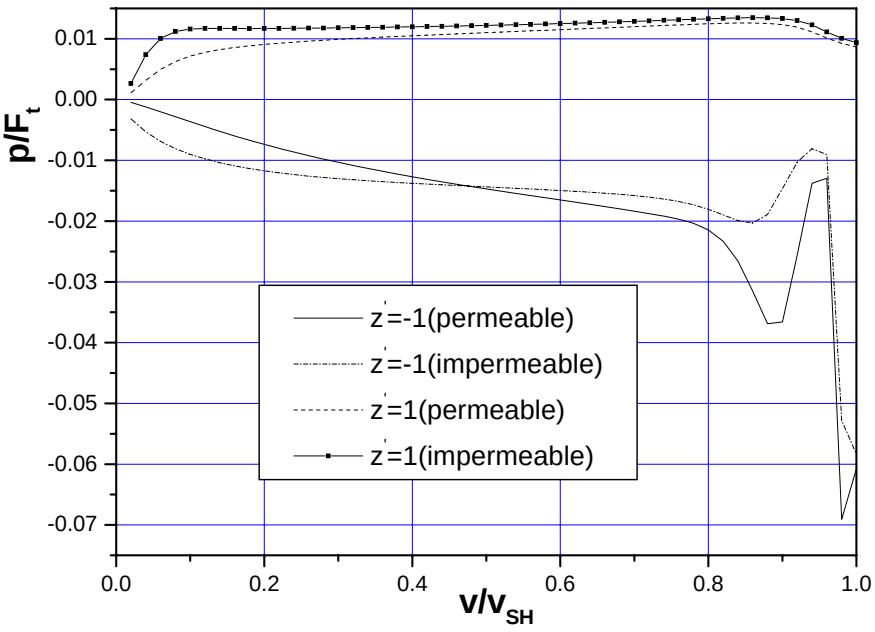

(d)

Figure 7: Dynamic response of two points with $z' = -1.0, 1.0$ and $\rho = 1.5$ near a permeable or impermeable circular tunnel subjected to a moving tangent concentrated ring load F_t with velocity ranging from $v/v_{SH} = 0.0$ to $v/v_{SH} = 1.0$: (a) radial displacement u_r / F_t; (b) axial displacement u_z / F_t; (c) hoop stress $\sigma_{\theta\theta} / F_t$; (d) pore pressure p / F_t.

5 Conclusions

Closed form solutions in the frequency-wave-number domain for a circular tunnel subjected to a moving load have been derived in the paper. The time-space domain solutions are obtained by analytical inverse Fourier transformation with respect to frequency together with numerical inverse Fourier transformation with respect to axial wave number. Our solutions are useful for design of subway tunnels embedded in saturated porous media. Also, our solution can be used in the evaluation of dynamic responses of mines to detonation waves. More importantly, the present solution can be used to check various numerical methods addressing moving load problems of tunnels or boreholes. Numerical calculations in our paper show moving loads have very complicated effects on the dynamic response of the porous medium. In summary, moving loads with high speed tend to generate larger displacement, stress and pore pressure than a static or lower speed loads do. In particular, when the velocity of a moving load approaches the velocities of the body waves of a porous medium, the response of the porous medium will increase significantly and exhibit an oscillating nature. In addition, the influence of the boundary condition depends on the location of receiver points and the load velocity. Generally, the boundary conditions along tunnel surface have a larger influence on stresses and pore pressure than on the displacements.

Acknowledgments

The research is financed by National Natural Science Foundation of China in the framework of the project No. 50578071. The helpful comments from the anonymous reviewers are greatly acknowledged.

References

Biot MA. Theory of propagation of elastic waves in a fluid-saturated porous solid, I, Low frenquency range. J. Acoust. Soc. Am. 1956, 28: 168-178.

Biot MA. Theory of propagation of elastic waves in a fluid-saturated porous solid, II: Higher frenquency range. J. Acoust. Soc. Am. 1956, 28: 179-191.

Biot MA. Mechanics of deformation and acoustic propagation in porous media. J. Appl. Phys. 1962, 33: 1482-1498.

Biot MA. General theory of three-dimensional consolidation. J. Appl. Phys. 1941, 12:155-164.

Burke M, Kingsbury HB. Response of poroelastic layers to moving loads. Int J Solids Struct 1984, 20(5):499–511.

Cui L, Cheng AHD, Abousleiman Y. Poroelastic solution for an inclined borehole. Journal of Applied Mechanics 1997, 64: 32-38.

Eason G. The stresses produced in a semi-infinite solid by a moving surface force. Int. J. Engng. Sci. 1965, 2: 581-609.

Fryba L. Vibration of solids and structures under moving loads. London: Thomas Telford, 1999.

Gonzalez JA, Abascal R. Linear viscoelastic boundary element formulation for steady state moving loads. Engineering Analysis with Boundary Elements 2004, 28: 815-823.

Grundmann H, Lieb M, Trommer E. The response of a layered halfspace to traffic loads moving along its surface. Arch Appl Mech 1999; 69(1):55–67.

Jin B, Yue ZQ, Tham LG. Stresses and excess pore pressure induced in saturated poroelastic halfspace by moving line load. Soil Dynamics and Earthquake Engineering 2004, 24: 25-33.

Johnson DL, Koplik J, Dashen R. Theory of dynamic permeability and tortuosity in fluid-saturated porous-media. J. Fluid Mech. 1987, 176: 379-402.

Jordan DW. The stress wave from a finite cylindrical explosive source. J Math. Mech. 1962, 11(4): 503-551.

Metrikine AV, Vrouwenvelder ACWM. Surface ground vibration due to a moving train in a tunnel: two-dimensional model. J. Sound Vib. 2000, 234(1):43–66.

Parnes R. Response of an infinite elastic medium to traveling loads in a cylindrical bore. Journal of Applied Mechanics 1969, 36: 51-58.

Parnes R. Steady-state ring-load pressure on a borehole surface. Int. J. Solids Structures 1986, 22: 73-86.

Parnes R. Elastic response to a time-harmonic torsion-force acting on a bore surface. Int. J. Solids Structures 1983, 19: 925-934.

Pride SR, Morgan FD, Gangi AF. Drag forces of porous-medium acoustics. Phys. Rev. B 1993, 47: 4964-4978.

Rajapakse RKND. Stress analysis of borehole in poroelastic medium. Journal of Engineering Mechanics 1993, 119: 1205-1227.

Rasmussen KM, Nielsen SRK, Kirkegaard PH. Boundary element method solution in the time domain for a moving time-dependent force. Computers and Structures 2001, 79: 691-701.

Siddharthan R, Zafir Z, Norris GM. Moving load response of layered soil. I. Formulation. J Engng Mech, ASCE 1993, 119(10):2052–71.

Appendix

The three constants $A(\omega,\xi)$, $B(\omega,\xi)$, $C(\omega,\xi)$ for a moving concentrated ring normal load F_n are given as follows

$$A(\omega,\xi)=\frac{F_n}{\Pi(\xi,\omega)}\delta(\omega+\xi v)\gamma_t H_0^{(2)}(\gamma_s R)H_1^{(2)}(\gamma_t R)(k_f^2-k_s^2)k_s^2(\alpha-k_s^2\varepsilon_1+\varepsilon_2)(\xi^2-\gamma_t^2) \tag{A.1}$$

$$B(\omega,\xi)=-\frac{F_n}{\Pi(\xi,\omega)}\delta(\omega+\xi v)\gamma_t H_0^{(2)}(\gamma_f R)H_1^{(2)}(\gamma_t R)k_f^2(\alpha-k_f^2\varepsilon_1+\varepsilon_2)(\gamma_t^2-\xi^2) \tag{A.2}$$

$$\begin{aligned}C(\omega,\xi)=&\frac{2i\xi F_n}{\Pi(\xi,\omega)}\delta(\omega+\xi v)(\gamma_s H_0^{(2)}(\gamma_f R)H_1^{(2)}(\gamma_s R)k_f^2(\alpha-k_f^2\varepsilon_1+\varepsilon_2)\\&-(\alpha+\varepsilon_2)\gamma_f k_s^2+H_0^{(2)}(\gamma_s R)H_1^{(2)}(\gamma_f R)+\varepsilon_1\gamma_f k_s^4 H_0^{(2)}(\gamma_s R)H_1^{(2)}(\gamma_f R))\end{aligned} \tag{A.3}$$

$$\begin{aligned}\Pi(\xi,\omega)=&\gamma_t(-2\gamma_f k_s^2 H_0^{(2)}(\gamma_s R)\,H_1^{(2)}(\gamma_f R)(k_t^2 H_1^{(2)}(\gamma_t R)\\&-2\xi^2\gamma_t R H_0^{(2)}(\gamma_t R))\mu(\alpha-k_s^2\varepsilon_1+\varepsilon_2)\\&+H_0^{(2)}(\gamma_f R)(2\gamma_s k_f^2 H_1^{(2)}(\gamma_s R)(-2\xi^2\gamma_t R H_0^{(2)}(\gamma_t R)\\&+k_t^2 H_1^{(2)}(\gamma_t R))\mu(\alpha-k_f^2\varepsilon_1+\varepsilon_2)\\&-R H_0^{(2)}(\gamma_s R)H_1^{(2)}(\gamma_t R)(2\xi^2-k_t^2)(2\mu\gamma_f^2 k_s^2(\alpha-k_f^2\varepsilon_1+\varepsilon_2)\\&+k_f^4\varepsilon_1(2\mu\gamma_s^2+\lambda k_s^2)-k_f^2(2\mu\gamma_s^2(\alpha+\varepsilon_2)+\lambda\varepsilon_1 k_s^4))))\end{aligned} \tag{A.4}$$